COSMIC RADIATION ISSUES FOR GRAVITATIONAL EXPERIMENTS IN SPACE

Saps Buchmant and Y. Jafry‡
† *W. W. Hansen Experimental Physics Laboratory, Stanford University, Stanford, U.S.A.*
‡ *Space Science Department of ESA, ESTEC, Noordwijk, The Netherlands.*

ABSTRACT

We discuss the disturbances caused by cosmic radiation on the test masses used for gravitational experiments in space. Experiments being considered are Gravity Probe B (GP-B), the Space Test of the Equivalence Principle (STEP), and the Laser Interferometer Space Antenna (LISA). The main disturbance effects are: charge deposition by particles stopping in the test masses, torque and momentum transfer, heating caused by energy deposition, and trapped flux motion in superconducting films. Charging is the main disturbance, requiring active compensation in order to meet the goals of gravitational experiments. The GP-B charge measurement and control system is completed, and has demonstrated the capability to limit the charge of gyroscopes to less than 10 pC. Non-contact charge measurement methods include the force modulation of the position or feedback control effort of the test masses, and charge evaluation using data from particle detectors. These charge measurement and compensation techniques are applicable to STEP and LISA. All other disturbances caused by cosmic radiation on the drag free test masses of these experiments are shown to be either small or manageable with appropriate experimental techniques.

I. INTRODUCTION

Testing gravitational theories requires an environment as free of disturbing forces as possible, with space becoming the new frontier where this class of experiments is being performed. Test masses on sattelites flying on Earth or Solar orbits benefit from both the ultralow gravity and the lack of seismic disturbances. However, disturbances caused by light pressure, residual gases, and micro-particles make precision gravitational measurements impossible, thus necessitating the use of drag free techniques[1] in order to further reduce the environmental disturbances. In a drag free experiment the test mass is placed in an isolated vacuum enclosure near the center of mass of the spacecraft. Thruster systems compensate for disturbances exerted on the spacecraft by maintaining its position with respect to the free floating test mass, therefore ensuring that the test mass will follow an inertial trajectory.

A number of residual disturbances limit the ultimate performance of drag free test masses. The leading disturbances are due to the forces exerted by the drag free sensing instrumentation, to variations in the mass distribution of the spacecraft and the test masses, to dissipative mechanisms caused by gas and surface phenomena, and to penetrating cosmic radiation impacting the test masses. In this paper we discuss the effects caused by radiation. Section II contains a brief description of the principal gravitational experiments with drag free test masses. In section III we discuss the cosmic radiation background and the disturbances it causes on the test masses. Sections IV to VI cover the experimental and analytical work which provides the solutions to these problems.

II. GRAVITATIONAL EXPERIMENTS IN SPACE USING DRAG FREE TEST MASSES

Three major space tests of gravitational theories are presently in progress. The Relativity Experiment Gravity Probe B (GP-B)[2] is a test of the rotational effects of gravity. GP-B will measure the geodetic and frame dragging relativistic rotational precessions by comparing the local frame of reference in a 650 km polar orbit, as determined by high precision electrostatically suspended cryogenic (~2 K) gyroscopes, with the fixed frame of reference of the distant stars, as determined by a telescope.

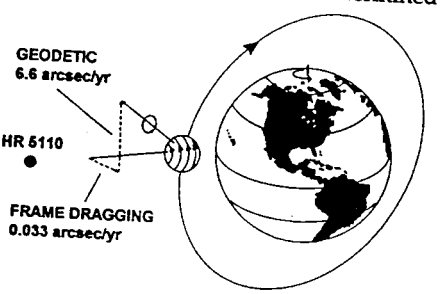

Figure 1. GP-B experimental concept

Figure 1 represents schematically the Relativity Mission experiment. In General Relativity the magnitudes of the geodetic and frame dragging precessions are 6.6 arcsec/yr and 0.033 arcsec/yr. The primary goals of the Relativity Mission are to measure frame dragging to better than 4×10^{-3} and the geodetic precession to better than 2×10^{-5}. The PPN parameter γ will be measured to 3×10^{-5} or better.[3] For a gyroscope in the GP-B drag free mode of less than 10^{-9} m/s^2, the residual non relativistic drift is about 0.02 marcsec/yr.

LISA, the Laser Interferometer Space Antenna,[4] is a Michelson interferometer placed in space and designed to detect gravitational waves. Three identical spacecraft, located at the vertexes of an equilateral triangle of 2×10^6 km on the side, define the two primary arms and the redundant arm of the interferometer. The constellation is placed in a

heliocentric orbit, 1 AU from the Sun, and 20° behind the Earth, while the three spacecraft move relative to each other in a circular orbit inclined at 60° to the ecliptic.

Each spacecraft contains drag free reference mirrors, which define the interferometer cavity, and two 30 cm aperture telescopes, pointing at the neighboring spacecraft, and used for transmitting and receiving the phase-locked 1064 nm Nd:YAG laser beams. The operational temperature of the drag free mirrors is between 200 and 250 K. Figure 2 represents schematically the LISA configuration. The LISA mission objective is the detection of gravitational radiation in the frequency range of 10^{-4} to 10^{-1} Hz, with a strain sensitivity of $4\times10^{-21}/\sqrt{\text{Hz}}$ at 10^{-3} Hz. Residual disturbance forces on the drag free reference mirrors must be limited to 10^{-15} m·s^{-2} in the measurement frequency band.

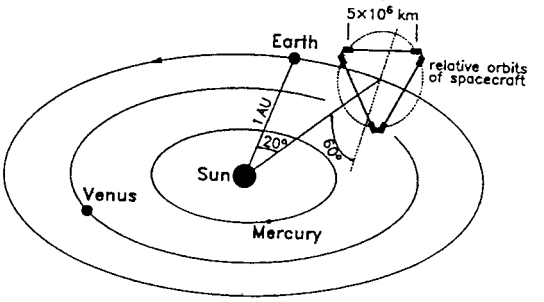

Figure 2. LISA experimental concept

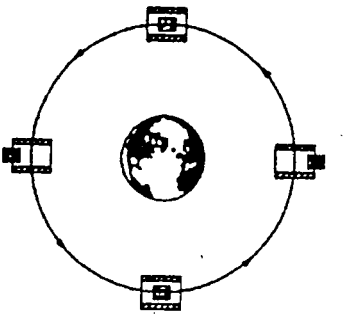

Figure 3. STEP experimental concept

STEP, the Space Test of the Equivalence Principle,[5] is designed to test the equivalence of the inertial and gravitational masses to 10^{-17}, an improvement of six orders of magnitude over the present results obtained by ground based experiments. Differential cryogenic (~2 K) accelerometers, each containing two cylindrically symmetric and concentric test masses made of different materials, are placed in a drag free trajectory, in Earth orbit, at 550 km altitude and 97°inclination.

Linear bearings and sensing circuits constrain the relative motion of the two test masses to a one dimensional motion. Violation of the equivalence principle would result in a differential acceleration of the test masses, and consequently their relative displacement at orbital frequency. Figure 3 shows the STEP experiment principle. Under drag free control the residual acceleration noise on the test masses is required to be less than or equal to 10^{-13} m·s^{-2} in the measurement bandwidth.

III. COSMIC RADIATION BACKGROUND AND DISTURBANCE EFFECTS

GP-B and STEP are exposed to three main sources of radiation: charged particles trapped in the Earth's magnetic belts, particles generated in solar flares, and galactic cosmic radiation. LISA in its heliocentric orbit is evidently not sensitive to particles in the Earth field. Figure 6 shows the daily orbit-averaged integral flux of protons and electrons for the GP-B orbit, 650 km altitude and 90° inclination. The trapped particle flux is given by the NASA/NSSDC models[6] AP-8 for protons and AE-8 for electrons, while the solar proton flux[7] is the yearly averaged median for the year 2000, the projected GP-B flight date. Due to its lower orbit, 550 km, the trapped particle flux for STEP is lower by

roughly a factor of two than the GP-B flux at 650 km altitude. The main contributions to the radiation environment in these orbits are the charged particles trapped in the Earth's magnetic field and the charged particles generated by solar flares. Radiation effects are caused principally by protons, as the shielding provided by the spacecrafts stops most electrons.

Galactic cosmic rays have much lower fluxes than the trapped particles and the solar flares. They contain, however, highly energetic heavy ions, and represent the main radiation source for LISA during periods of low solar activity. Figure 5 shows the relative ion abundance in cosmic radiation as a function of the nuclear charge number Z.

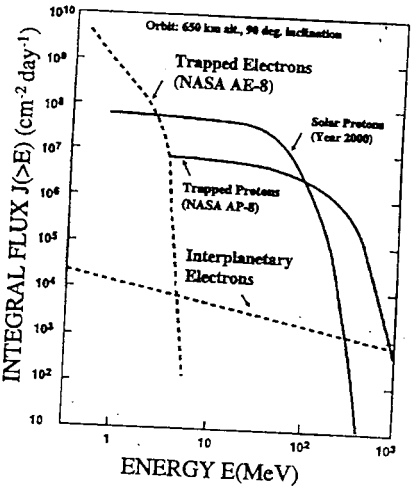

Figure 4. Cosmic radiation background for the GP-B satellite.

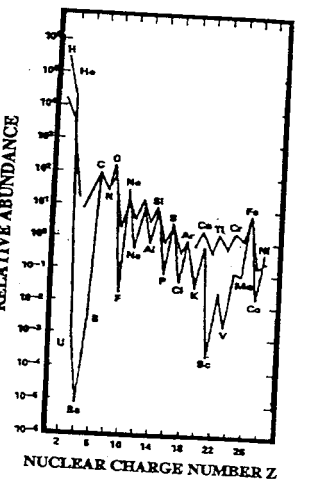

Figure 5. Relative abundance of cosmic rays versus charge number Z.

Radiation causes four major disturbance effects on drag free test masses: a) Ionizing radiation deposits energy in the test masses, causing heating. This effect is important for the cryogenic experiments, GP-B and STEP, but can be neglected for LISA. b) Primary cosmic rays and secondary emission charged particles deposited in the test masses cause their charging, and represent potentially a major source of error for all the experiments under consideration. Non contact charge measurement and compensation techniques, developed for GP-B, have been tested to be effective in mitigating the disturbances caused by charging on free floating test masses.[8] The same techniques will be utilized for charge control for LISA and STEP. c) Momentum transferred to and torques exerted by radiation on the test masses represent a second major class of disturbances affecting all three experiments and necessitating careful analysis to estimate the errors they cause. d) GP-B incorporates superconducting thin films in its gyroscopes. Local heating by energetic ions can cause the movement of flux vortices trapped in these films.

The energy, charge, and momentum transferred to the test masses were calculated by two methods: analytically, using the Bethe-Bloch formula, and by Monte Carlo simulation, using the European Space Agency's GEANT radiation transport code. The results agree in within the calculation errors of about 15%, and confirm that all effects of cosmic radiation on the test masses are due mainly to protons and heavy ions.

IV. HEATING

Test masses, floating freely in the ultrahigh vacuum environment, required by the precision of the experiments, can only dissipate the heating produced by cosmic radiation via black body radiation. Note that even at the GP-B and STEP operating temperature and pressure of 2.5 K and 10^{-9} Pa, the thermal conductivity of the residual gas is small compared to thermal radiation.

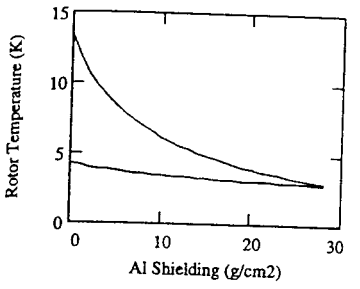

Figure 6. Heating of GP-B rotor

Figure 6 shows the calculated temperature, in K, for the GP-B gyroscope, as a function of the shielding depth, in g/cm^2 of Aluminium, for two cases: heating from trapped protons in the lower trace, and heating from an anomalously large solar flare in the upper trace. Radiation shielding for the GP-B gyroscope rotors is about 20 g/cm^2 Aluminium equivalent, in order to reduce heating and charging. The rotor temperature will be 3.6 K, (1.1 K above the housing temperature), for the maximum expected 1 nW heat input and an emissivity coefficient of 0.03. A three day major solar flare will raise the rotor temperature to only 5.5 K, safely below its 9 K superconducting transition. Without radiation shielding the temperatures would be 4 K and 10 K respectively. Note that an effective thermal emissivity coefficient of less than 0.5% would result in the heating of the rotor to above its superconducting temperature, an unacceptable experimental condition.

Table I gives the temperature increases of the inner and outer test masses for STEP as a function of the orbit altitude. The calculations are for a single pass through the South Atlantic Anomaly (SAA), the area of lowest magnetic field which accounts for most of the trapped radiation exposure. These temperature increases are well within the temperature stability requirements for STEP.[9] During major solar flares the STEP measurement can be discontinued and the test masses brought into equilibrium with the thermal bath, a possibility which does not exist in the case of the fast spinning (170 Hz) GP-B gyroscopes. Heating from radiation is not a problem for LISA, where the operating temperature is 200-250 K.

Table I. Temperature increase (mK) for STEP test masses for a single passage through the SAA as a function of orbit altitude (km)

Orbit Altitude (km)	350	400	450	500	550	600	650
Outer Mass Temp. Increase (mK)	0.14	0.31	0.63	1.17	1.96	3.24	5.01
Inner Mass Temp. Increase (mK)	0.12	0.29	0.58	1.08	1.81	3.01	4.68

The coefficient of thermal emissivity for the Niobium coated gyroscope rotors of the GP-B experiment has been measured directly using a Titanium radiator matching the thermal emissivity of the gyroscope housing.[10] This calorimetric measurement has a sensitivity of 100 pW. The effective combined thermal emissivity of a gyroscope rotor and a Titanium housing was measured to be 3.0 ± 0.5%.

V. CHARGING

Table II summarizes the maximum allowable charge on the test masses of each of the experiments, as well as a range of approximate durations required to reach that charge.[8,9,11,12] The time needed to reach maximum charge varies depending on solar activity.

Table II. Maximum allowable charge on the test masses and the time needed to reach it

Experiment	Orbit	Max. Charge (C)	Time to max. charge (h)
GP-B	650 km, 90°	$\leq 10^{-11}$ C	3-300
LISA	1AU Solar	$\leq 5\times10^{-14}$ C	1-10
STEP	550 km, 97°	$\leq 10^{-13}$ C	1-10

Figure 7 shows the calculated charging rates, in fA, of the GP-B gyroscopes versus the shielding depth, in g/cm^2, of Aluminium for two cases: charging from trapped protons (lower trace), and charging from an anomalously large solar flare (upper trace).

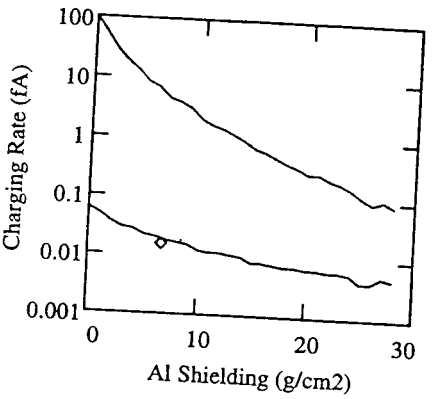

Figure 7. Charging of GP-B rotors

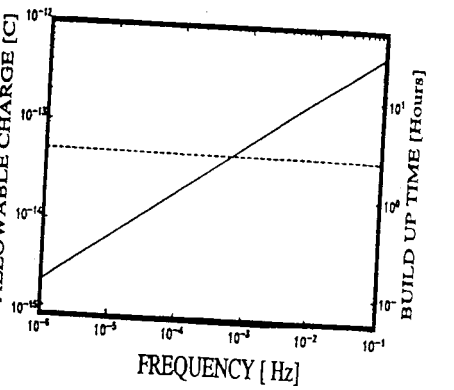

Figure 8. Allowable charge for LISA

The diamond represents the result of a Monte Carlo simulation with the GEANT code. A calculation of the allowable charge for LISA is shown in figure 8. The left axis gives the limit on the allowable charge due to Lorentz disturbances, in C, while the right axis is the time needed to reach this limit in the presence of cosmic rays. The dashed line is the limit on the allowable charge due to the interaction with the electrostatic servo forces applied to the test mass.

Figure 9 gives the results of a Monte Carlo simulation of the charging of the outer test mass of STEP as a function of the shielding thickness in cm of Tungsten. The full curves represent the charging due to the SAA, in altitude steps of 50 km, while the broken curve shows the charging caused by cosmic rays. All the results are for the solar minimum activity. These results make it clear that active charge measurement and control are necessary for all three experiments.

We propose two methods, one direct and one indirect, for the non-contact measurement of small amounts of charge. In the direct method a modulated electrostatic

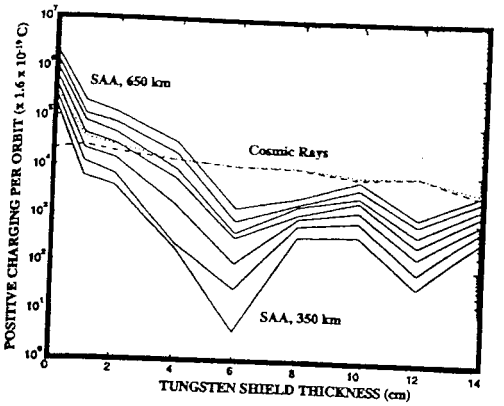

Figure 9. Charging of STEP outer test mass

force is applied equally and out of phase to opposite sides of the test mass resulting in its motion or in the change in drag free control effort proportional to the charge.[8] The indirect method uses information from particle monitors to calculate the charge deposited on the test masses. While more accurate, the direct method has the disadvantage of applying disturbing forces to the test mass. This problem can be minimized by using low duty cycle for the direct measurement, possibly in conjunction with the particle monitoring method, in order to ensure continuous charge measurement. GP-B uses the force modulation method to measure the rotor charge achieving an accuracy of better than 4 mV for an integration time of 100 s, while the particle monitoring method will be used as a backup. LISA and STEP are planning to use the same charge measurement methods.

For charge compensation GP-B utilizes electrons generated by photoemission from both the rotor and its housing. These electrons are added to or removed from the rotor using a dedicated biasing electrode.[8] Development testing for GP-B has proven these charge measurement and control techniques, and the flight system is presently under construction. An alternative source of electrons for charge compensation, utilizing field emission cathodes, is presently being developed. This simpler more robust system could be used in STEP and LISA.

VI. MOMENTUM TRANSFER, TORQUES, AND TRAPPED FLUX MOTION

Table III summarizes the calculated expected momentum transfer and torques for GP-B, LISA, and STEP. Upper limits for the disturbance levels allowed by the experimental error budgets are included in bold italics. LISA and STEP are relatively insensitive to torques. In all cases the expected disturbances caused by radiation are well below the error budgets.

Table III. Expected and allowable momentum transfer and torques from radiation

	GP-B	LISA	STEP
Momentum Transfer from Radiation ($m \cdot s^{-2}$)	$\leq 10^{-14}$	$\leq 10^{-18}/\sqrt{Hz}$	$\leq 10^{-17}$
Allowable Momentum Transfer ($m \cdot s^{-2}$)	$\leq 10^{-8}$	$\leq 10^{-16}/\sqrt{Hz}$	$\leq 10^{-16}$
Torque Transfer from Radiation (N·m)	$\leq 10^{-20}$	N/A	N/A
Allowable Torque Transfer (N·m)	$\leq 10^{-17}$	*N/A*	*N/A*

GP-B incorporates thin superconducting films in the gyroscope. Local heating of the 3 μm niobium coating of the rotor by protons can cause trapped flux motion, and thus sturb the readout system. Modeling the heating as an instantaneous line source, we lculate the maximum motion of a fluxon to be about 0.1 μm, and the number of flux

jumps to be approximately 10 per year. This is well below the level of 10^3 flux jumps per year which would double the readout error. LISA and STEP do not utilize superconducting films in their test masses.

VII. CONCLUSIONS

We conclude that all disturbances caused by radiation in space on the drag free test masses of the gravitational tests, GP-B, LISA, and STEP, have experimental solutions fully demonstrated by the work on GP-B. Heating of the cryogenic test masses is balanced by thermal radiation cooling, the critical parameter being the effective thermal emissivity. For the GP-B rotors, it is measured to be about 3%, well in excess of the required 1%. Charging of the test masses is a problem for all these experiments. Charge management, using measurement by force modulation and electrons generated by ultraviolet photoemission, are the solutions for the GP-B gyroscope charging problem. Alternative and complementary techniques for GP-B are the indirect charge measurement method using particle monitors and electron generation by field emission cathodes. A combination of these techniques will ensure the charge management for LISA and STEP. Momentum transfer and torques generated by radiation have been calculated and simulated to be well below the level allowed in the error budgets for all three experiments. Finally, the trapped flux motion induced by protons in the superconducting thin film coating of the GP-B rotors causes disturbances two orders of magnitude below the allowed level.

ACKNOWLEDGMENTS

This work was supported by NASA contracts NAS8-39225 and NRA 95-OSS-09. We wish to thank Anna Muza and Denise Freeman for editorial assistance.

REFERENCES

1) Staff of Space Dept. Johns Hopkins Univ. and Staff of Guidance and Control Lab. Stanford Univ., Journal of Spacecraft **11**, 637 (1974).
2) J. P. Turneaure, C. W. F. Everitt, B. W. Parkinson, Advances in Space Research **9**, 29 (1989).
3) C.W.F. Everitt and Saps Buchman, *Particle Astrophysics Atomic Physics and Gravitation*, pp 467 (Editions Frontieres, Cedex-France, 1994)
4) D. Hils, P.L. Bender, and R.F. Webbink, Astrophys. J. **360**, 75 (1990).
5) P.W. Worden Jr., A Cryogenic Test of the Equivalence Principle, PhD thesis, Stanford University, Stanford, California (1974).
6) J. I. Vette, *The NASA/National Space Science Data Center Trapped Radiation Environment Model Program (1964-1991)*, NSSDC/WDC-A-R&S 91-29, (1991).
7) J. Feynman, G. Spitale, J. Wang, and S. Gabriel, Journal of Geophysical Research 98, 13281 (1993).
8) Saps Buchman, T. Quinn, G.M. Keiser, D. Gill and T.J. Sumner, Rev. Sci. Instrum. 66, 120 (1995)
9) *STEP, Report on the Phase A Study*, ESA NASA SCI (93) 4, (1993).
10) Robert Brumley, Saps Buchman, and John Mester, Czechoslovak Journal of Physics **46-S5**, 2875 (1996)
11) *LISA, Pre-Phase A Report*, ESA (1995).
12) Y. Jafry, T.J. Sumner, and Saps Buchman, Classical and Quantum Gravity **13-11A**, A97 (1996).